



Non-linear Correlation Between Transient Photoconductivity Parameters and Light Intensity of $\text{Ge}_{20}(\text{Te}_{35}\text{Se}_{65})_{80}$ Glass

F. Abdel-Wahab² · I. M. Ashraf^{1,2} · Fatma B. M. Ahmed²

Received: 21 July 2021 / Accepted: 13 December 2021 / Published online: 3 January 2022
© The Minerals, Metals & Materials Society 2022

Abstract

An investigation of photoconductivity in bulk glass of $\text{Ge}_{20}(\text{Te}_{35}\text{Se}_{65})_{80}$ prepared by a melt-quenching method is described. The measurements were carried out at room temperature and at different levels of illumination. The I – V data have been detected to be straight lines for all intensities, which specify ohmic conduction. Intensity (F) dependence of the photocurrent demonstrates nearby power law dependence of the photocurrent on incident radiation. The photosensitivity was found to increase with increasing light intensity. Both the life time and the differential life time decrease with increasing the intensity of the light. The differential life time and the life time are represented by nonlinear fitting by the exponential function. This behavior can be well interpreted in terms of the photo-induced effect. New localized states (recombination of localized electrons and holes) are induced in the band gap due to prolonged strong photo illumination. Thermal measurement reveals that the present glass is a good glass former.

Keywords Photocurrent · life time · differential life time · photo-induced effect · glass former

Introduction

Chalcogenide semiconducting glasses are recognized as heavy-anion glasses having sulfur (S), selenium (Se), and tellurium (Te) as the core elements of their configurations.¹ The chalcogen element, Se, is supposed to be a stimulating substance due to its significant technical applications.² The addition of the other chalcogen element, Te, can create and increase the disorder and increase the thermal stability. The addition of a third element, such as gallium (Ga), tin (Sn), thallium (Tl), and germanium (Ge) has been found to develop the physical properties of ternary Se-Te glass.^{3–6}

In recent years, chalcogenide glasses have had a well-defined potential in developments in technology, due to their unique electrical, optical, and tunable properties, for photoconductive applications.^{7–9} Photoconductivity investigations^{10–16} on chalcogenide glasses have gained great attention due to their basic and technological properties in

numerous solid-state devices. Chalcogenide glasses are categorized by the occurrence of localized states in the mobility gap and the absence of long-range order.

It is well known that the photocurrent in these materials is organized by carrier localization and delocalization routes.¹⁷ The photoconductivity has been confirmed to be an appropriate method in the recognition of the origin of recombination which, in turn, offers information about the localized states in these materials, and sheds light on the photosensitivity of the substances for device applications.

Most photoconductivity studies have been carried out on evaporated glass films, but only a few on bulk glasses. Sharma¹⁶ investigated the photoconductive properties of thin films of $\text{Ge}_{20}\text{Te}_{80-x}\text{Sbx}$ ($x = 0$ at%, 2 at%, 4 at%, 6 at%, and 10 at%) and showed that the dark activation energy, the optical band gap, and photosensitivity were decreased with increasing the concentration of antimony. Photocurrent versus light intensity follows the power law and the dominance of bimolecular recombination was found. Znaidia et al.¹⁸ studied the photoconductivity within the temperature (T) range 300–420 K for thermally evaporated thin films of $\text{Ge}_5\text{As}_{22}\text{Te}_{73-x}\text{In}_x$ (where $x = 0$ at%, 3 at%, 6 at%, and 9 at%). The current density was found to be directly proportional to the applied electric field which indicating ohmic behavior. It was found that the dark and photoconductivity

✉ Fatma B. M. Ahmed
Fatmaowny@sci.aswu.edu.eg

¹ Department of Physics, College of Science, King Khalid University, Abha, Saudi Arabia

² Department of Physics, Faculty of Science, Aswan University, Aswan, Egypt

increased with increasing the In content. With increasing the In content from 0 at% to 9 at%, the peak of the photocurrent moved to a lower energy with a corresponding decrease in the E_g value from 1.1 eV to 0.9 eV. Iaseniuc and Iovu¹⁹ reported the experimental results of the steady-state photoconductivity of amorphous single-layer structures (Al-As_{0.40}S_{0.30}Se_{0.30}-Al, Al-Ge_{0.09}As_{0.09}Se_{0.82}-Al, and Al-Ge_{0.30}As_{0.04}S_{0.66}-Al) and of an amorphous heterostructure (Al-As_{0.40}S_{0.30}Se_{0.30}/Ge_{0.09}As_{0.09}Se_{0.82}/Ge_{0.30}As_{0.04}S_{0.66}-Al). A complex structure for the photocurrent spectra was shown which was attributed to the various values of the optical band gap of the amorphous layers ($E_g \approx 2.0$ eV for As_{0.40}S_{0.30}Se_{0.30} and Ge_{0.09}As_{0.09}Se_{0.82} and $E_g \approx 3.0$ eV for Ge_{0.30}As_{0.04}S_{0.66}). El-Denglawey et al.²⁰ studied the dark and photoconductivity for Ag-mixed Se₇₀Te₃₀ thermally deposited thin films, and found that at 300 K the dark conductivity was increased, whereas the activation energy for the dark, photo and thermal response was decreased with increasing the Ag content.

Selenium and tellurium are the most often used chalcogens and are potentially utilized in several electronic devices. The addition of Ge to the Se-Te matrix extends their potential applications, since the addition of Ge strengthens the average bond in the system and enhances the glass formation. In the present work, the authors have decided to choose a new bulk Ge₂₀(Te₃₅Se₆₅)₈₀ composition as a promising system for advanced photodevices, and to investigate its steady state and transient photocurrent, as well as the effect of the illumination level on the photosensitivity and life time. We furthermore have attempted to interpret our experimental data in the frame of predictions of photo-induced effects.

Experimental Details

Bulk Ge₂₀(Te₃₅Se₆₅)₈₀ chalcogenide glass was prepared by the conventional melt-quenching method using high-purity elements, Se, Te, and Ge. About 8 g of the batch was transferred into a quartz ampoule which was evacuated to a pressure of 1.3×10^{-6} kpa. The ampoule was kept in a controlled muffle furnace at 950°C for 9 h with regular shocking to confirm the complete homogeneity of the melt. Quenching was then achieved in ice water.

In order to identify the amorphous nature of the sample, x-ray diffraction measurements were performed using a Philips diffractometer type 1710 with a Ni-filtered Cu K α source ($\lambda = 0.154$ nm). The thermal behavior was investigated using a differential scanning calorimeter (DSC; TA 2010). Typically, 15 mg of the sample in powder form was sealed in standard aluminum pans and heated at a rate of $25^\circ\text{C min}^{-1}$ in the temperature range 25–600°C.

A portion, 3 mm in length and $5 \text{ mm}^2 \times 1.5 \text{ mm}^2$ in area, was cut from the ingot, and the surface was polished

to be mirror-like. The sandwich configuration was used to measure the dark and under-illumination currents. Au paste was used to make a good ohmic contact for electrical measurements in the sample. The sample was fixed inside the optical cryostat (Oxford optistat DN1704), and the measurements were carried out at room temperature and in a vacuum of 1.3×10^{-4} kpa. A programmable electrometer (Keithley 6517b) was employed as a direct current power supply in addition to measuring the current. A tungsten lamp (1000 W) was used to illuminate the sample.

Results and Discussion

Figure 1 shows the x-ray diffraction pattern of the Ge₂₀(Te₃₅Se₆₅)₈₀ glass. It is obvious that the glass is amorphous which is defined by the presence of a low-intensity broad peak in the pattern.

Figure 2 shows a representative DSC curve acquired when the chalcogenide Ge₂₀(Te₃₅Se₆₅)₈₀ specimen was heated at a rate of 25°C/min . Four distinguishing parameters are determined in the studied temperature range. The first one is a small endothermal outcome corresponding to the glass transition temperature ($T_g = 130^\circ\text{C}$), the second is the onset temperature of crystallization ($T_c = 342^\circ\text{C}$), the third is the peak temperature of crystallization ($T_p = 414^\circ\text{C}$), and the fourth is the melting temperature ($T_m = 485^\circ\text{C}$). It is useful to use the previous characteristic temperatures to evaluate the glass-forming ability (GFA) which is considered to be an essential issue in operating the examined materials in various applications. Hrubý²¹ introduced a parameter H_f which can be used as the index of the GFA:

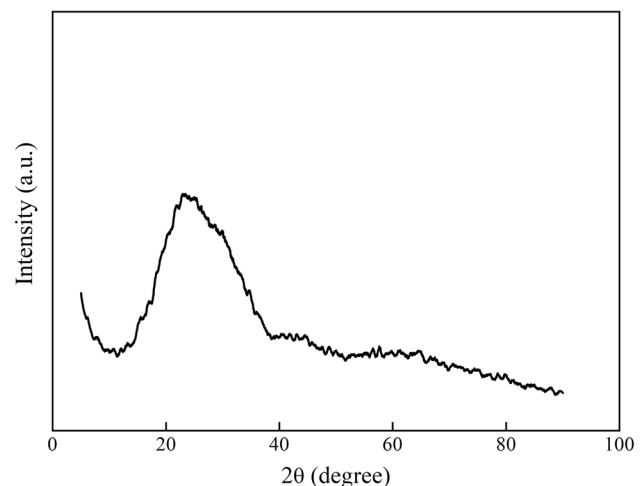


Fig. 1 X-ray diffraction pattern of the prepared Ge₂₀(Te₃₅Se₆₅)₈₀ glass.

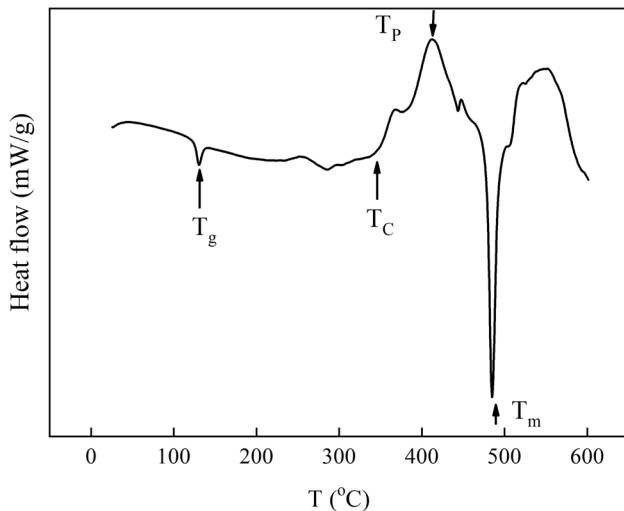


Fig. 2 A representative DSC curve for the $\text{Ge}_{20}(\text{Te}_{35}\text{Se}_{65})_{80}$ chalcogenide glass.

$$H_r = \frac{T_c - T_g}{T_m - T_c} \quad (1)$$

Note that the H_r parameter accumulates the nucleation and growth sides of the phase transformation where greater values of $T_c - T_g$ postponement of the nucleation progression and the small values of $T_m - T_c$ delay the growth procedure of the nucleated crystals. According to Hrubý, when $H_r \leq 0.1$ it is difficult to form glass, whereas with $H_r \geq 0.5$, glass can be readily formed with adequate cooling rates. In this study, the value of H_r for the $\text{Ge}_{20}(\text{Te}_{35}\text{Se}_{65})_{80}$ glass was calculated to be 1.48, which is greater than the H_r value of Se-Te glass which is reported to be about 0.27.^{3,22} This further means that $\text{Ge}_{20}(\text{Te}_{35}\text{Se}_{65})_{80}$ is a good glass former.

Steady-state photoconductivity of bulk chalcogenide $\text{Ge}_{20}(\text{Te}_{35}\text{Se}_{65})_{80}$ was studied at room temperature using white light. The I - V curves at various illumination levels are depicted in Fig. 3. The electric field across the sample is presumed to be uniform. The plots of the I - V data have been detected to be straight lines for all intensities, which evidently specify the ohmic conduction. The slope of the I - V curves varies with illumination levels. The increase in the slope is small for lower intensities (0–300 Lux), and it gets larger for high intensities i.e. (1780–4250 Lux). The slope at 4250 Lux has been detected to be nearly eight times that at 0 Lux. This can be attributed to the increase in the charge carriers' density as the number of incident photons increase.

In order to examine the kinetics of the carrier recombination process in $\text{Ge}_{20}(\text{Te}_{35}\text{Se}_{65})_{80}$, the relationship between the intensity and steady-state photocurrent has been examined. The intensity dependence of photocurrent is shown in Fig. 4. The plots of $\ln(I_{\text{ph}})$ versus $\ln(F)$ at different applied

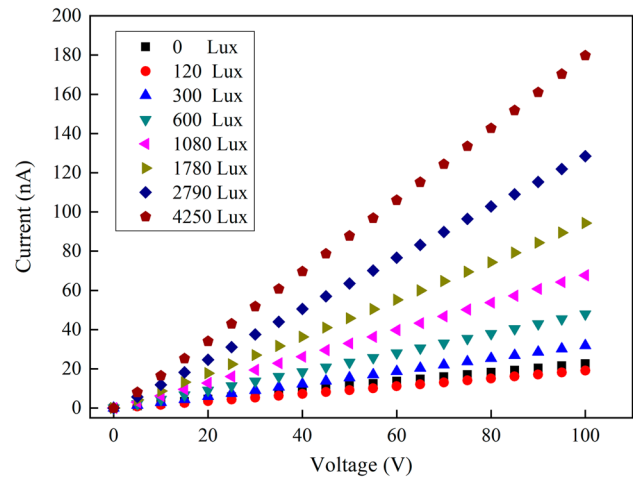


Fig. 3 The I - V curves at various illumination levels.

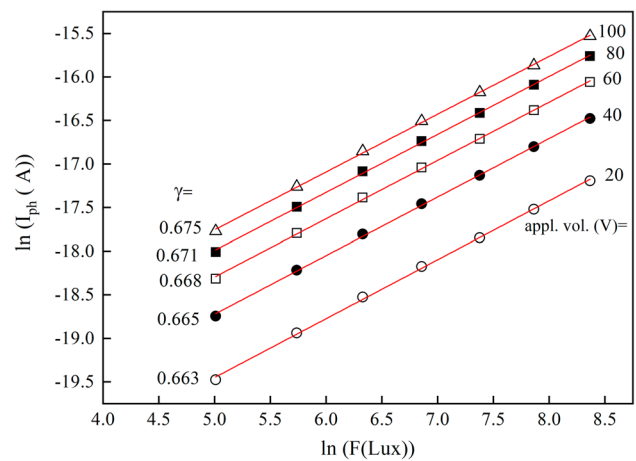


Fig. 4 The variation of room-temperature photocurrent (I_{ph}) with intensity (F) at different applied voltages.

voltages have been considered. It is obvious from this figure that the relationship is following the power law: $I_{\text{ph}} \propto F^\gamma$, where γ is the exponent and its value can be determined by the recombination mechanism.²³ For the present sample, γ is approximately 0.67 with the little systematic variations. Rose²⁴ suggests that, when the value of γ is equal to 0.5, the recombination process is bimolecular recombination, and, while the value of γ is equal to 1.0, this indicates monomolecular recombination. However, in the situation of continuous distribution of traps, the value of γ may be somewhere between 0.5 and 1.0 depending on the intensity and the temperature range. The value $\gamma = 0.67$ is designated to the occurrence of a continuous distribution of localized states in the mobility gap.

The significant factor in photoconductivity measurements is the photosensitivity $S = [I_{\text{ph}}/I_d]$ of a particular substance,

which determines the quality of the material to be used in photoconductive tools. We have, as a result, calculated S at room temperature for $Ge_{20}(Te_{35}Se_{65})_{80}$. The consequences of these calculations are depicted in Fig. 5 as open circles. It is evident from this figure that the photosensitivity increases with increasing light intensity. The solid curve is the non-linear fit to experimental data and obeys the following relation $S \propto F^{0.62}$.

Transient photoconductivity has been investigated via exposing the sample to light with instantaneous recording of the current for a given period. Subsequently, the light was switched off and the decay of current was recorded. The outcomes of transient photoconductivity measurements, i.e., photocurrent versus time plots for $Ge_{20}(Te_{35}Se_{65})_{80}$ at room temperature for different illumination levels are shown in Fig. 6. It is obvious from the figure that the initial growth and decay of currents are fast and afterward the progress becomes slow. The decay of photocurrent as shown in Fig. 6 can be elucidated by means of the differential life time (τ_d) concept (which is also defined as decay time constant). Quantitatively, the decay time constant is given as²⁵:

$$\tau_d = -I_{ph}(\max) \left(\frac{dI_{ph}}{dt} \right)^{-1} \tag{2}$$

where dI_{ph}/dt is the decay rate and $I_{ph}(\max)$ is the value of photocurrent with which the decay starts. Figure 7a and b shows the dependence of the differential life time and the life time on the light intensity. Note that the life time was calculated at the beginning of the decay of the photocurrent. Both the life time and the differential life time decrease with increasing the intensity of the light. Increasing the intensity

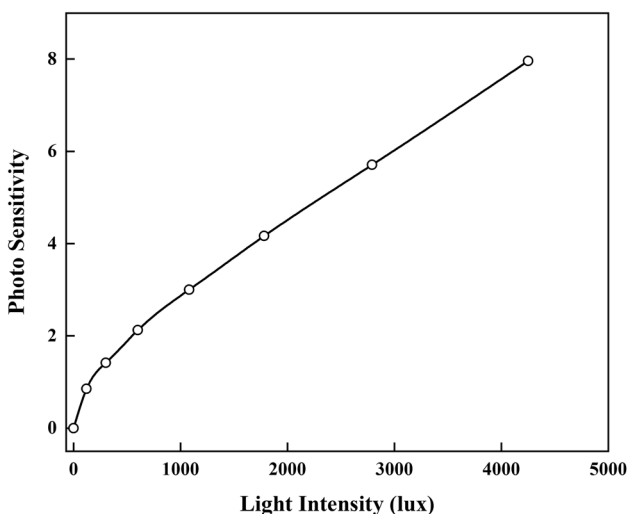


Fig. 5 The variation of photosensitivity of $Ge_{20}(Te_{35}Se_{65})_{80}$ glass with light intensity.

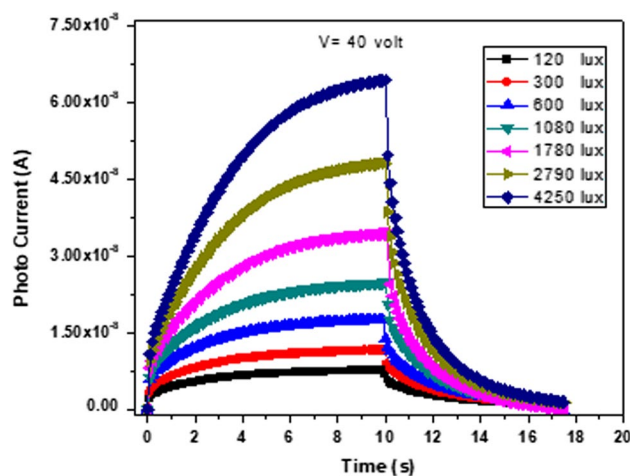


Fig. 6 Rise and decay photocurrent with time for $Ge_{20}(Te_{35}Se_{65})_{80}$ at room temperature at different illumination levels.

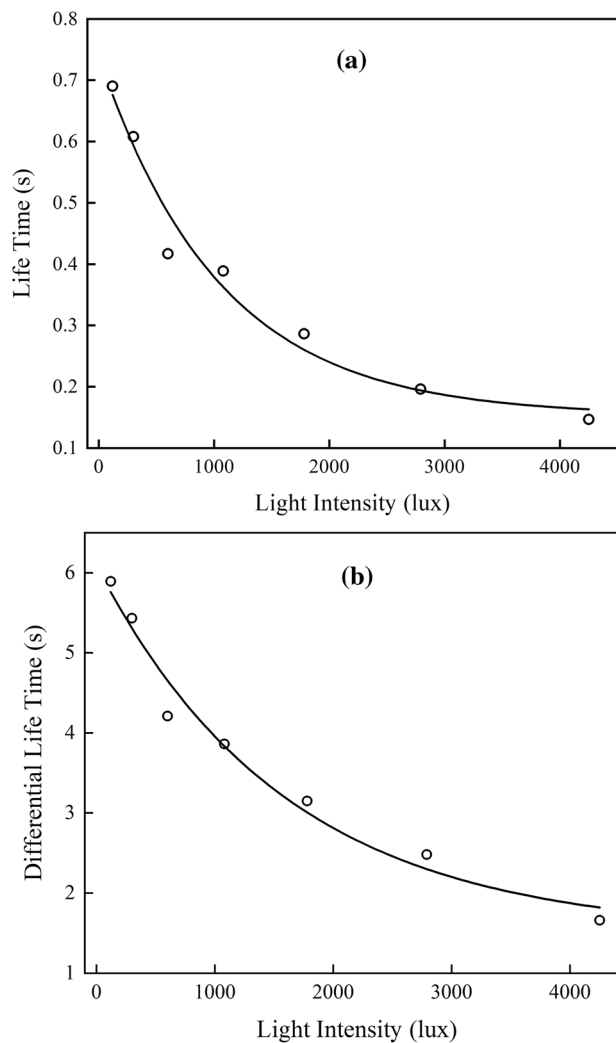


Fig. 7 (a) Variation of the life time with light intensity; (b) variation of the differential life time with light intensity.

Table 1 The obtained physical parameters from nonlinear fitting for both τ_d and τ using Eq. 3

	Life time (s)	Differential life time (s)
y_0 (s)	0.153 ± 0.041	1.5 ± 0.46
A_1 (s)	0.587 ± 0.048	4.59 ± 0.41
β	1049 ± 259	$15,981 \pm 435$

of light leads to more traps, which reduces the life time of the current carriers.

Next, we examine the differential life time (τ_d) and the life time (τ) by nonlinear fitting. Both the τ_d and τ are presented by the following exponential function:

$$y = y_0 + A_1 \exp(-I/\beta) \quad (3)$$

where A_1 is a constant (equal to the total quantity of variation), y_0 is the total quantity at the largest intensity, β is assumed to be a certain constant value, being inversely proportional to the incident illumination, and y is the measured value (τ_d and τ) at light intensity I . The physical parameters of Eq. 3 obtained from the fitting of τ_d and τ are presented in Table 1.

The physical interpretation for the behavior of τ and τ_d with the intensity can be understood in the framework of a photo-induced effect. Commonly, this effect includes volume change, photo-darkening, photo-bleaching, defect creation, and photo-melting. Photo-induced phenomena occur when chalcogenide samples are subjected to band gap illumination.²⁶ The magnitude of this changes when the effect rises, and is expected to depend on the intensity as well as the wavelength of light. Several studies have been carried out in order to offer an elucidation of the photo-induced phenomena.^{26–30} On the other hand, the photo-induced effect yields a degradation in the dark and photo-conductivities in chalcogenide glasses.³¹ The origin of these degradation phenomena is supposed to be associated with the photo-induced creation of some types of defects. In fact, Biegelsen and Street³² found that a new electron spin resonance signal can be detected during strong and long-time illumination, and they proposed that these new localized states are nearby pairs of charged D+ and D- centers. When these centers are created, i.e., the density of recombination centers increases, the differential life time and the life time would decrease after strong illumination.

Conclusions

Bulk $\text{Ge}_{20}(\text{Te}_{35}\text{Se}_{65})_{80}$ chalcogenide glass was prepared by the conventional melt-quenching method. The H_r value for the $\text{Ge}_{20}(\text{Te}_{35}\text{Se}_{65})_{80}$ glass was calculated to be 1.48, which

indicated that $\text{Ge}_{20}(\text{Te}_{35}\text{Se}_{65})_{80}$ is a good glass former. The I - V curves at various illumination levels have been detected to be straight lines for all intensities, which evidently specifies ohmic conduction for the glass sample. The relationship between intensity (F) and room-temperature photocurrent (I_{ph}) at different applied voltages is straight lines with the slope (γ) being approximately 0.67 with little systematic variation. The value $\gamma = 0.67$ is designated to the occurrence of a continuous distribution of localized states in the mobility gap. The photosensitivity increases with increasing light intensity according to the following relation $S \propto F^{0.62}$. Both the life time and the differential life time decrease with increasing the intensity of the light. The differential life time and the life time are represented by nonlinear fitting by the exponential function ($y_0 + A_1 \exp(-I/\beta)$).

Acknowledgments The author I.M. Ashraf extends his appreciation to the Deanship of Scientific Research at King Khalid University for funding this work through the group's research program under Grant No. R.G.P.1/216/41

Conflict of interest The authors declare that they have no conflict of interest.

References

1. K. Tanaka, and K. Shimakawa, *Amorphous Chalcogenide Semiconductors and Related Materials* (Berlin: Springer, 2011).
2. J.A. Savage, Optical properties of chalcogenide glasses. *J. Non-Cryst. Solids* 47, 101 (1982).
3. F. Abdel-Wahab, Observation of phase separation in some Se-Te-Sn chalcogenide glasses. *Physica B* 406, 1053 (2011).
4. A. El-Korashy, A. Bakry, M.A. Abdel-Rahim, and M. Abd El-Sattar, Annealing effects on some physical properties of $\text{Ge}_5\text{Se}_{25}\text{Te}_{70}$ chalcogenide glasses. *Phys. B Condens. Matter* 391, 266 (2007).
5. E.M. Ahmed, N.A. El-Ghamaz, and F. Abdel-Wahab, Structural, thermal, electrical, and negative resistance properties of $(\text{Se}_{60}\text{Te}_{40})_x\text{Tl}(100-x)$ chalcogenide glasses. *Phys. Status Solidi (A)* 215, 1700666 (2018).
6. F. Abdel-Wahab, A. Merazga, M.S. Rasheedy, and A.A. Montaser, Optical characterization of the annealing effect on $\text{Ge}_5\text{Te}_{20}\text{Se}_{75}$ thin films by variable angle of-incidence spectroscopic ellipsometry. *Optik* 127, 3871 (2016).
7. V.S. Shiryaev, and M.F. Churbanov, Trends and prospects for development of chalcogenide fibers for mid-infrared transmission. *J. Non-Cryst. Solids* 377, 225 (2013).
8. J.L. Adam, and X. Zhang, *Chalcogenide Glasses: Preparation, Properties and Applications* (Sawston: Woodhead, 2014).
9. C. Goncalves, M. Kang, B.U. Sohn, G. Yin, J. Hu, J. Hu, D.T. Tan, and K. Richardson, New candidate multicomponent chalcogenide glasses for supercontinuum generation. *Appl. Sci.* 8, 2082 (2018).
10. K. Shimakawa, A. Yoshida, and T. Arizumi, Photoconduction of glasses in the Te-Se-Sb system. *J. Non-Cryst. Solids* 16, 258 (1974).
11. E.A. Fagen, and H. Fritzsche, Photoconductivity of amorphous chalcogenide alloy films. *J. Non-Cryst. Solids* 4, 480 (1970).
12. A.S. Maan, D.R. Goyal, and A. Kumar, Steady-state photoconductivity and decay kinetics in thin films of a-In₂₀Se₈₀. *J. Non-Cryst. Solids* 110, 53 (1989).

13. G. Mathew, K.N. Madhusoodanan, and J. Philip, Characteristics of photoconductivity in amorphous $\text{Ge}_x\text{Sb}_{10}\text{Se}_{90-x}$ thin films. *Phys. Status Solidi (A)* 168, 239 (1998).
14. P.Z. Saheba, S. Asokanc, and K.A. Gowdab, Transient and steady state photoconductivity studies on bulk glasses and amorphous films of Ge-Te-Pb-Composition and spectral dependence. *J. Optoelectron. Adv. Mater.* 5, 1215 (2003).
15. M. Kamboj, and F. Mohammadi, Steady state and transient photoconductivity measurements in $a\text{-Se}_{90}\text{-xSb}_{10}\text{In}_x$ thin films. *Thin Solid Films* 518, 1585 (2009).
16. I. Sharma, Temperature-dependent photoconductive properties of Ge-Sb-Te thin films. *Phase Transit.* 92, 851 (2019).
17. D.L. Staebler, and C.R. Wronski, Optically induced conductivity changes in discharge-produced hydrogenated amorphous silicon. *J. Appl. Phys.* 51, 3262 (1980).
18. S. Znaidia, I. Kebaili, I. Boukhris, R. Neffati, H.H. Smailly, H. Algarni, and A. Dahshan, Impact of indium content on the thermoelectric power, dark conductivity, and photoconductivity of Ge-As-Te thin films. *Appl. Phys. A* 126, 1 (2020).
19. O. Iaseniuc, and M. Iovu, Absorption and photoconductivity spectra of amorphous multilayer structures. *Beilstein J. Nanotechnol.* 11, 1757 (2020).
20. A. El-Denglawey, P. Sharma, P. Kumar, E. Sharma, D.C. Sati, K.A. Aly, and A. Dahshan, Dark, photo and thermally driven conductivity of Ag-mixed $\text{Se}_{70}\text{Te}_{30}$ semiconducting thin films for thermoelectric applications. *J. Mater. Sci. Mater. Electron.* 32, 25074 (2021).
21. A. Hrubý, Evaluation of glass-forming tendency by means of DTA. *Czechoslov. J. Phys. B* 22, 1187 (1972).
22. M.A. Abdel-Rahim, A. Gaber, A.A. Abu-Sehly, and N.M. Abdela-zim, Crystallization study of Sn additive Se-Te chalcogenide alloys. *Thermochim. Acta* 566, 274 (2013).
23. R.H. Bube, *Photoelectrical Properties of Semiconductors* (Cambridge: Cambridge University Press, 1992).
24. A. Rose, *Concepts in Photoconductivity and Allied Problem* (New York: Krieger, 1978), p. 38.
25. W. Fuhs, and J. Stuke, Hopping recombination in trigonal selenium single crystals. *Phys. Status Solidi (B)* 27, 171 (1968).
26. K. Shimakawa, A. Kolobov, and S.R. Elliott, Photoinduced effects and metastability in amorphous semiconductors and insulators. *Adv. Phys.* 44, 475 (1995).
27. H. Fritzsche, Photo-induced fluidity of chalcogenide glasses. *Solid State Commun.* 99, 153 (1996).
28. A.V. Kolobov, H. Oyanagi, K. Tanaka, and K. Tanaka, Structural study of amorphous selenium by in situ EXAFS: observation of photoinduced bond alternation. *Phys. Rev. B* 55, 726 (1997).
29. X. Zhang, and D.A. Drabold, Direct molecular dynamic simulation of light-induced structural change in amorphous selenium. *Phys. Rev. Lett.* 83, 5042 (1999).
30. F. Abdel-Wahab, N.A. Karar, and A. Merazga, Time dependent bond arrangement approach to photo-induced changes in $\text{Ge}_{30}\text{-xSbxSe}_{70}$ thin films. *Mater. Chem. Phys.* 242, 122521 (2020).
31. K. Shimakawa, Persistent photocurrent in amorphous chalcogenides. *Phys. Rev. B* 34, 8703 (1986).
32. D.K. Biegelsen, and R.A. Street, Photoinduced defects in chalcogenide glasses. *Phys. Rev. Lett.* 44, 803 (1980).

Publisher's Note Springer Nature remains neutral with regard to jurisdictional claims in published maps and institutional affiliations.